EPJ Web of Conferences **38**, 03001 (2012)
DOI: 10.1051/epjconf/20123803001

Study of the γ decay of high-lying states in ^{208}Pb via inelastic scattering of ^{17}O ions

A. Bracco and F.C.L. Crespi

Dipartimento di Fisica dell'Università di Milano e INFN, I-20133 Milano, Italy

Abstract. High-lying states in ^{208}Pb nucleus were populated via inelastic scattering of a ^{17}O beam at bombarding energy of 20 MeV/u. Their subsequent gamma decay was measured with the detector system AGATA Demonstrator based on HPGe detectors, coupled to an array of large volume $LaBr_3$:Ce scintillators. Preliminary results in comparison with *(γ,γ')* data, for states in the 5-8 MeV energy interval, seem to indicate that in that region the states belong to two different groups one with a isoscalar character and the other with a isovector nature. This is similar to what was observed in other stable nuclei with *(α,α'γ)* experiments. The multipolarity of the observed gamma transitions is determined with remarkable sensitivity thanks to angular distribution measurements. Data aiming at studying the neutron decay of the Giant Quadrupole Resonance in the ^{208}Pb by the high resolution measurement of the following gamma decay are also presented in their preliminary form.

1 Introduction

The use of heavy ions inelastic scattering at approximately 20 MeV/u to study highly excited states (up to the region of the Giant Quadrupole Resonance) is a good tool when the measurement of the subsequent gamma decay is also performed with high resolution. Some partial results of the most recent experiments of this type, performed to investigate the electric-dipole ($E1$) response of nuclei at energies around the particle threshold, are reported in this contribution. The understanding of the electric-dipole response at energy around the binding energy is presently attracting considerable interest since the dipole strength distribution in that region affects considerably the reaction rates in astrophysical scenarios [1,2], where photodisintegration reactions are important. In addition the $E1$ strength is also interesting because it is expected to provide information on the neutron skin and thus on the symmetry energy of the equation of state [3-7]. The first evidence of an accumulation of low-lying $E1$ strength in heavy nuclei, larger than that due to the tail of the giant dipole resonance (GDR), dates back to early 70's [8]. However, only in recent years, experimental and theoretical investigations, on both stable and radioactive nuclei, revealed that this is a common phenomenon in most atomic nuclei [9-24]. The accumulation of E1strength around the particle separation energy is commonly denoted as pygmy dipole resonance (PDR) (see e.g.[5]) due to the much smaller size of its strength in comparison with the giant dipole resonance (GDR). The hydrodynamical model describes this pygmy strength as associated to the vibration of the neutron skin.

An interesting feature in the region of the pygmy resonance has been observed [25-29] in a number of different stable nuclei, by comparing results of photon-scattering and α scattering experiments. In particular, it has been found that one group of states is excited in both type of reactions, while another group of states at higher energies is only excited in the (γ,γ') case. These experimental findings are in qualitative agreement with different phonon models which predict a low-lying isoscalar component dominated by neutron-skin oscillations and a higher-lying group of states with a stronger isovector character associated to the tail of the giant dipole resonance.

The use of an additional probe as the inelastic scattering of ^{17}O at 20 MeV/u which has, similarly to alpha particles, a rather strong isoscalar character is expected to add valuable information on the quest of the nature of these low-lying $E1$ states.

In addition, with the same experiment we intended to study of the gamma and neutron decay of the Isoscalar Giant Quadrupole Resonance (ISGQR) in the 10-13 MeV range. In the past, inelastic scattering of ^{17}O ions at the energy of 22 MeV/u was used to study the gamma decay of the ISGQR of ^{208}Pb. The strength of the resonance and its coupling with low-lying collective states [30, 31] were obtained. However, the existing measurements were performed using low-resolution gamma-ray detectors. Although the presence of a fine structure superimposed on the broad bump of the ISGQR in ^{208}Pb has been

known for decades, only recently detailed investigations performed with *(e,e')* and *(p,p')* experiments provided evidence that this is indeed a global feature of the ISGQR over a wide range of nuclei, such as ^{166}Er, ^{120}Sn, ^{90}Zr, ^{89}Y, ^{58}Ni [32,33]. Different techniques have been used to extract the energy scales associated to the fine structure, [32-39]. Comparison with second-RPA calculations indicates that the energy scales can indeed arise from the first step of the damping mechanism, that is the coupling of the 1p-1h states to the 2p-2h states (see e.g. [32, 33]). This calls for additional high resolution investigations which are feasible using germanium detectors and also $LaBr_3$:Ce scintillator arrays for the gamma decay measurement.

The experiment described in this paper was made at LNL-INFN laboratory using the Tandem-ALPI accelerator complex [40].

In Sec. 2, a detailed description of the experimental technique and of the gamma and particle detection systems is given, while in Sec. 3 preliminary results of the experiment are discussed for the case of ^{208}Pb.

2 Experimental technique and setup

In this experiment an ^{17}O beam at the energy of 20 MeV/u in the laboratory frame, provided by PIAVE-ALPI accelerator system of the Legnaro National Laboratories [40], was used together with a ^{208}Pb target. In the upper panel of figure 1 a schematic illustration of the experimental setup is displayed. The choice of ^{17}O beam is motivated by the fact that this nucleus has a rather small neutron separation (i.e. 4.1 MeV). This property allows to avoid to have background in the gamma spectra at energy E> 4 MeV due to the projectile when one wants to investigate the gamma emission from the target excitation. In fact, if an excitation energy larger than 4.1 MeV is transferred to the projectile, the neutron emission channel becomes dominant and thus the outgoing nucleus becomes ^{16}O which is well separated by ^{17}O in the particle detector system.

The detection of the scattered ^{17}O ions was performed with two segmented ΔE-E silicon telescopes. These are pixel detectors having the geometrical features that are similar to those that will be employed for the future project TRACE [41], expecting to cover a large solid angle. The ΔE detectors were 200 μm thick, corresponding to an energy loss of about 70 MeV for an ^{17}O ion of 340 MeV (20 MeV/u). The E detectors were 1 mm thick. This last thickness is sufficient to stop the ^{17}O ions completely. Each detector is segmented in 60 pads of 4 x 4 mm^2, for an active area of 20 x 48 mm^2. The large active area provides a good solid angle coverage.

The main feature of these detectors is the identification in charge and mass the scattered ions. In addition the excitation energy transferred to the target nucleus is measured with medium resolution (1.2-1.5 MeV). An example of a two-dimensional histogram displaying the Total Kinetic Energy (TKE) of ^{17}O ions measured in one pad of the ΔE-E silicon telescopes versus the energy deposit measured in the ΔE pad is shown in figure 2. From this figure one sees a clear separation of the different oxygen isotopes.

A picture of the gamma-ray detection system is given in the bottom panel of figure 1. In this picture the gamma detectors are on the right side. The gamma detectors are part of two separated arrays: i) the AGATA (Advanced GAmma-ray Tracking Array) Demonstrator [42, 43], namely the first step of the new generation segmented HPGe gamma-ray spectrometer AGATA, and ii) an array of 8 large volume (3.5" x 8") $LaBr_3$:Ce scintillators from the HECTORplus array [44, 45]. These scintillators couple the best properties characterizing inorganic scintillators (high efficiency, subnanosecond time resolution) with an energy resolution surpassed only by that of germanium detectors.

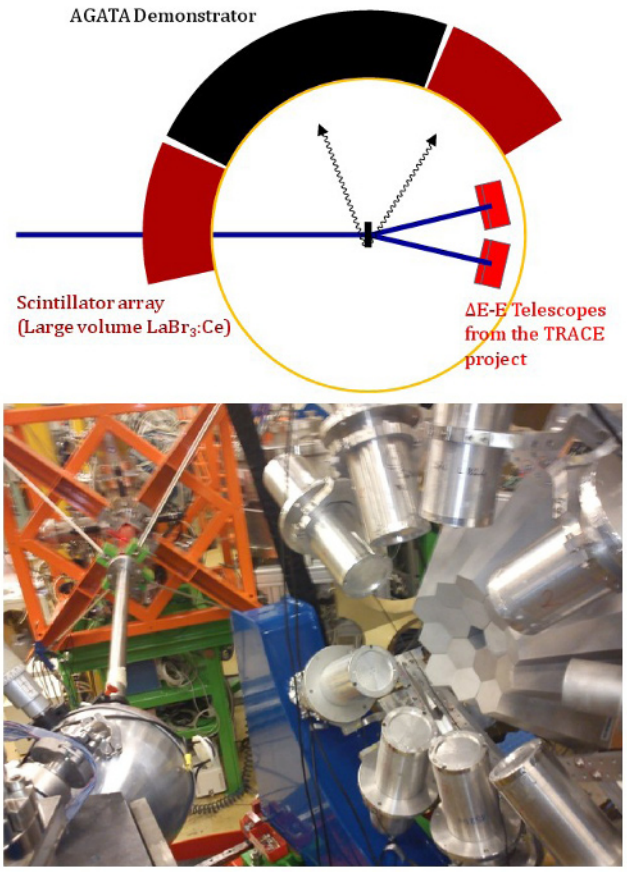

Fig. 1. Bottom panel: the detection systems used to measure gamma rays in the experiment (AGATA Demonstrator and $LaBr_3$:Ce array) are on the right side in the picture. Top panel: schematic representation of the experimental setup including silicon detectors at small angles (13 degrees) and the gamma detectors covering a wide angular range.

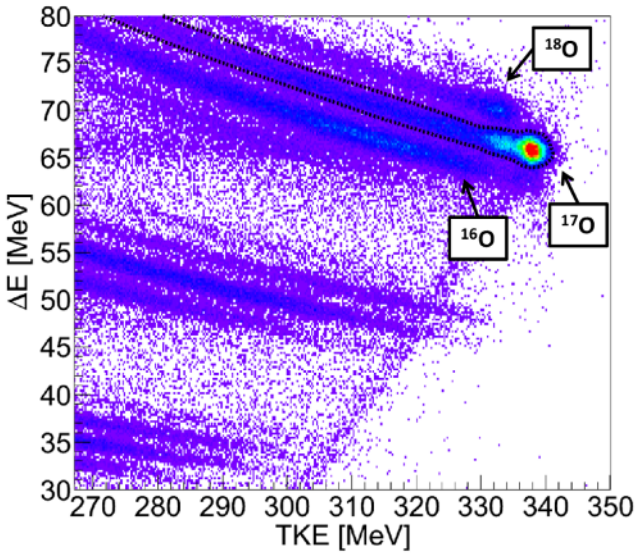

Fig. 2. Two-dimensional histogram of the Total Kinetic Energy (TKE) measured in one pad of the TRACE telescopes versus the energy deposit measured in the ΔE pad. The dotted line shows the separation of the oxygen isotopes.

3 Preliminary results

In the analysis of the experiment the information from the Si telescopes is used not only for the selection of the reaction channel but also for the correlation of the gamma-ray energy with the excitation energy transferred to the target nuclei. This quantity can be measured with the Total Kinetic Energy Loss (TKEL) of the projectile, which is the difference between the Total Kinetic Energy (TKE) measured in an event and the energy corresponding to an elastic scattering event. The gamma spectrum obtained with the AGATA Demonstrator after selecting the inelastically scattered ^{17}O events is shown (in blue) in the upper panel of figure 3, together with the spectrum (in red) obtained with the additional requirement that the energy of the gamma rays equals the TKEL values within a window ±1.5 MeV wide. By examining these two spectra it is evident that this TKEL condition enhances the relative intensity of the ^{208}Pb gamma-ray transitions at 2615 keV (3^-) and at 4085 keV (2^+), with respect to the background. In the bottom panel of figure 3 the same spectra described above, in this case for the $LaBr_3$:Ce scintillator array, are displayed. The high resolution data obtained with AGATA show (see upper panel of figure 3) that the 4085 keV gamma line is splitted in two components. This splitting originates from Doppler shift due to the ^{208}Pb target nuclei recoil motion and the two components are associated to events in which the ^{17}O scattered ions are detected by the left/right silicon telescope, respectively. The speed of the recoils is of the order of 0.5% of the speed of light. While this value appears quite small it is enough to cause a shift of more than 10 keV for high-energy gamma rays.

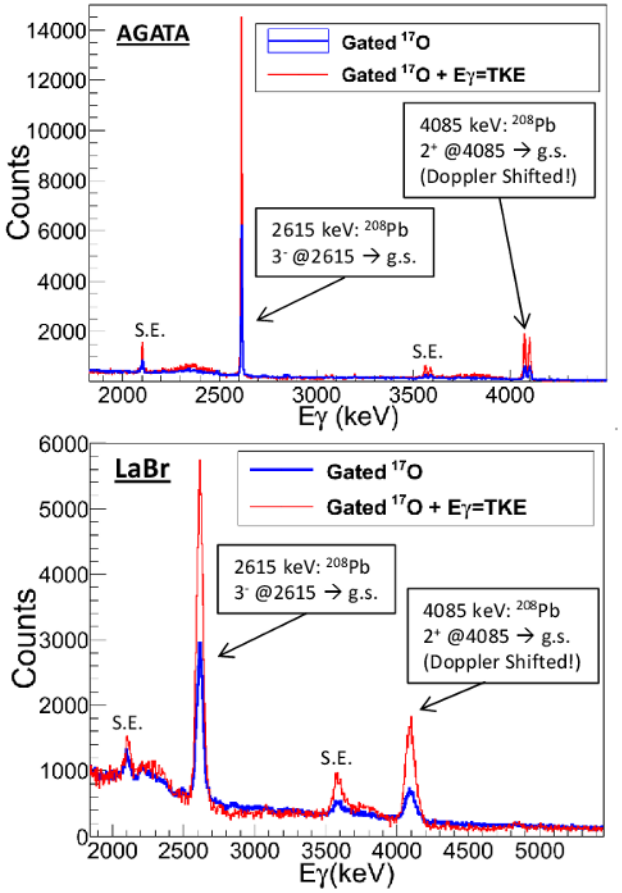

Fig. 3. Upper panel: gamma spectra measured with the AGATA Demonstrator, under different gating conditions: the blue spectrum is gated on the ^{17}O scattering channel, while the red spectrum has the additional requirement that the energy equals the TKEL within a ±1.5 MeV large window. The spectra are normalized to the total number of counts. Bottom panel: same as above panel but here the data are from the used $LaBr_3$:Ce scintillator array.

In order to perform a Doppler correction for the recoil, we calculated, with simple kinematics considerations, the velocity vector of the recoil associated to each pad of the silicon telescopes. The gamma emission direction was determined instead using the position information from AGATA detectors. The results of this procedure are shown in figure 4, where the AGATA spectra before (black line) and after (red line) Doppler correction are compared. As can be seen the splitting of 4085 keV gamma line is correctly removed once the Doppler correction is performed.

Although the gamma-ray spectrum in the 5-8 MeV energy range is dominated by *E*1 transitions, some *E*2 transitions are also present (this is also known from previous Nuclear Resonance Fluorescence experiments [46,47]). It is then important to have the possibility to separate the two contributions through the different angular distribution of the emitted gamma rays. In the case of the AGATA Demonstrator it is possible to measure the emission direction of each gamma ray with a

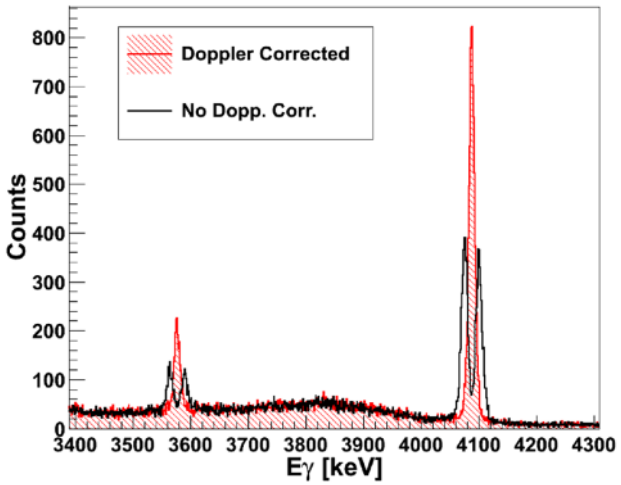

Fig. 4. Comparison of AGATA gamma spectra before (black line) and after (red line) the Doppler correction for the ^{208}Pb recoil motion is applied. The splitting of 4085 keV gamma line is correctly removed once the Doppler correction is performed.

remarkable precision (~ 1°), thanks to the Pulse Shape Analysis and tracking algorithms. We considered for each event the angle ($\theta_{\gamma,recoil}$) between the gamma-ray emission direction and the ^{208}Pb recoil velocity vector (reconstructed using the information from the silicon telescope pad which detected the ^{17}O ion). Figure 5 shows the angular distribution obtained for the 4085 keV line. The measured variation in intensity ($W(\theta_{\gamma,recoil})$) as a function of the angle is well reproduced with the expected trend for the *E*2 transition in ^{208}Pb (2^+ @ 4084 keV → g.s.).

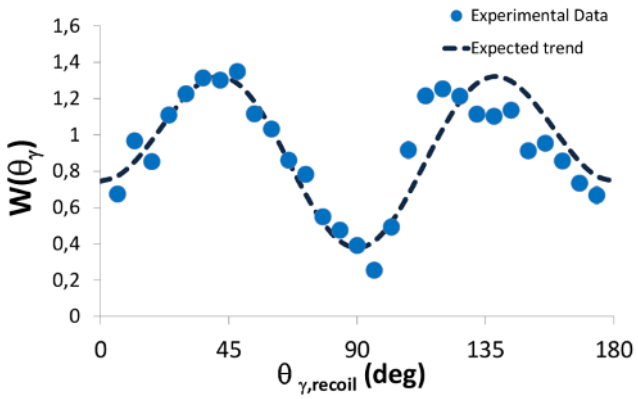

Fig. 5. The light-blue dots display, for the case of the 4085 keV line, the measured variation in gamma emission intensity ($W(\theta_{\gamma,recoil})$) as a function of the $\theta_{\gamma,recoil}$ angle (see text for description). The dotted line represents the expected trend for the *E*2 transition in ^{208}Pb (2^+ @ 4084 keV → g.s.).

Although the use of tracking algorithms greatly improves the Peak/Total ratio for the AGATA Demonstrator [29, 30], as compared to traditional HPGe arrays, still a significant number of counts in the spectra are associated to Compton events and to single/double escape events. This can be clearly seen, for example, in the AGATA spectra of figure 3 and figure 4. In order to remove from the spectrum line-shape the effect of such background, we applied the Compton unfolding techniques implemented in the RADWARE software package [48]. The response function of the AGATA Demonstrator was computed with GEANT4 [49, 50], for photon energies in the range from 1 MeV up to 15 MeV. The result of this unfolding procedure is shown in figure 6. In this last figure the original gamma spectrum is displayed in the upper panel (black line), while the blue spectrum in the bottom panel is after the unfolding. The removal of the Compton background and of the single escape peaks in the blue spectrum is evident. One can see in particular the single escape peaks removed around the 5715 keV line (indicated with a black arrow). The spectra in figure 6 are displayed in the 5-8 MeV energy interval, dominated by *E*1 transitions associated to the PDR mode in ^{208}Pb.

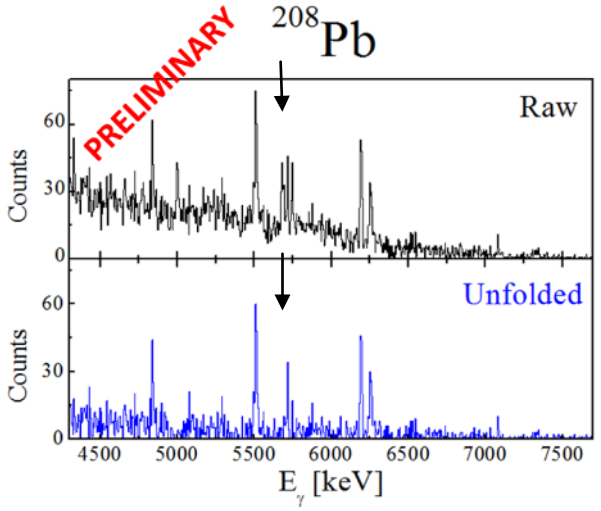

Fig. 6. AGATA gamma spectra obtained with the gating conditions described in the text and displayed in the 5-8 MeV energy range, dominated by *E*1 transitions. The original gamma spectrum is displayed in the upper panel (black line), while the blue spectrum in the bottom panel is after the unfolding.

A comparison of the experimental results with theoretical calculations requires the extraction of the B(*E*1) for each state of the resonance from the experimental cross-sections. In principle, the absolute cross-section obtained from the DWBA calculation should be compared to the experimental cross-section. We decided, however, to evaluate the relative strength of each state compared to a reference one, and scale all B(*E*1) values with the value for the reference state found in literature [32]. We used as a reference line the strongest *E*1 transition, at 5512 keV, using the value of B(*E*1) measured in [32]. In addition the energy dependence was deduced with DWBA calculations. Figure 7 displays the experimental values of the B(*E*1) of the PDR states in ^{208}Pb measured with our setup (in blue) and with the NRF technique (in green), convoluted with a Lorentzian curve with a width of 500 keV. There is a remarkable overlap between the two curves below ~6.5 MeV, while for higher energies there is an abrupt change in the response for the two different probes. This indicates that there is a splitting of the PDR

in ^{208}Pb similar to what has been observed for lighter nuclei with the *(α,α'γ)* technique [14-17]. The low-energy part of the resonance is excited equally well by heavy ions and photons, while the high-energy part is weakly excited by ions.

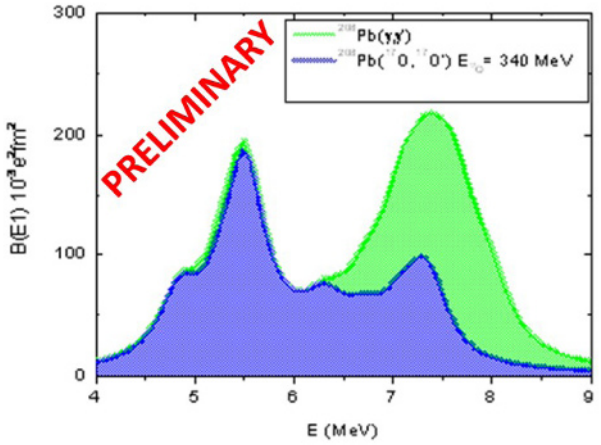

Fig. 7. Preliminary results for the experimental values of the B(*E*1) of the PDR states in ^{208}Pb extracted from data taken with our setup (in blue) and with the NRF technique (in red), convoluted with a Lorentzian curve with a width of 500 keV.

In order to study the neutron decay from the GQR and GMR region different region of excitation energy above the neutron binding energy were selected. In particular the gamma-ray spectra measured with the AGATA Demonstrator corresponding to the decay from high lying states (>7 MeV) are displayed in figure 8. The spectra of figure 8 are obtained by imposing different gating conditions on the Total Kinetic Energy Loss (TKEL) of the scattered ^{17}O projectile, detected in the silicon telescopes. The black spectrum in the upper panel displays the events associated to TKEL < 7 MeV, the red spectrum displays the events associated to a TKEL in the 10-13 MeV interval and finally the blue spectrum in the bottom panel displays the events associated to a TKEL in the 13-16 MeV interval. Gamma lines from ^{208}Pb, ^{207}Pb and ^{206}Pb are labeled in the figure indicating the associated transitions. An enhancement of gamma lines from ^{207}Pb and ^{206}Pb for the higher values of excitation energy is evident. This result opens the possibility to use the acquired data for the study of the neutron decay of the Giant Quadrupole Resonance in the ^{208}Pb nucleus.

4 Conclusions

The present study, although in its preliminary form, has shown an interesting result and an interesting opportunity related to a future analysis. The interesting result concerns the *E*1 response in the pygmy resonance region. Similarly to what was found using the *(α,α'γ)* reaction, also in this case the results seem to indicate that there are two groups of states one with a more isoscalar character and the other with a more isovector character. Data aiming at studying the neutron decay of the Giant Quadrupole Resonance in the ^{208}Pb by the high resolution measurement of the following gamma decay are also presented in their preliminary form. The future analysis of these data is expected to provide information on the neutron decay of the GQR and GMR with unprecedented resolution. The neutron decay is important to shed light on the damping mechanisms of giant resonances and to extract the direct decay component. This allows to test theory in detail.

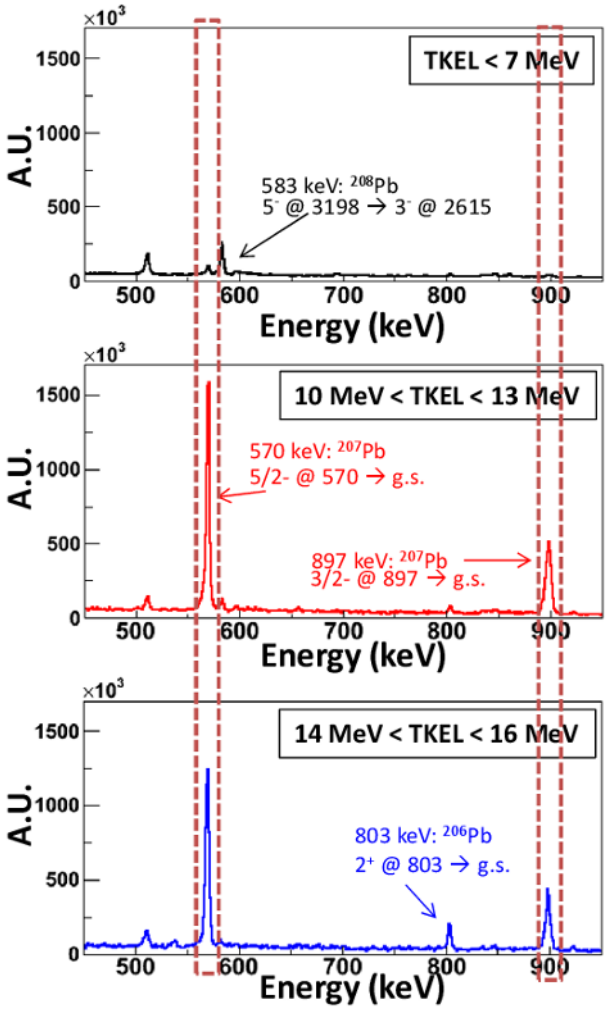

Fig. 8. Gamma spectra measured with the AGATA Demonstrator, obtained after imposing different gating conditions on the TKEL of ^{17}O ion detected in the silicon telescopes. In particular: the black spectrum in the upper panel displays the events associated to TKEL < 7 MeV, the red spectrum displays the events associated to a TKEL in the 10-13 MeV range and finally the blue spectrum in the bottom panel displays the events associated to a TKEL in the 14-16 MeV range. The three spectra are normalized to the total number of counts. Gamma lines from ^{208}Pb, ^{207}Pb and ^{206}Pb, enhanced after imposing the different gates on the TKEL, are labeled indicating the associated transitions.

References

1. S. Goriely, Phys. Lett. B **436**, 10 (1998)
2. S. Goriely, E. Khan, Nucl. Phys. A **706**, 217 (2002)
3. A. Carbone, *et al*., Phys. Rev. C **81**, 041301(R) (2010)
4. O. Wieland and A. Bracco, Prog. Part. Nucl. Phys. **66**, 374 (2011)
5. J. Piekarewicz, Phys. Rev. C **73**, 044325 (2006)
6. P.-G. Reinhard, W. Nazarewicz Phys. Rev. C **81**, 051303 (2010)
7. A. Klimkiewicz, *et al*., Phys. Rev. C **76**, 051603 (2007)
8. G.A. Bartolomew, *et al*., Adv. Nucl. Phys. **7**, 229 (1973)
9. O. Wieland, *et al*., Phys. Rev. Lett. **102**, 092502 (2009)
10. T. Hartmann, *et al*., Phys. Rev. Lett. **93**, 192501 (2004)
11. A. Leistenschneider, *et al*., Phys. Rev. Lett. **86**, 5442 (2001)
12. E. Tryggestad, *et al*., Phys. Lett. B **541**, 52 (2002)
13. P. Adrich, *et al*., Phys. Rev. Lett. **95**, 132501 (2005)
14. D. Vretenar, *et al*., Nucl. Phys. A **692**, 496 (2001)
15. L. Cao and Z. Ma, Mod. Phys. Lett. A **19**, 2845 (2004)
16. N. Paar, *et al*., Rep. Prog. Phys. **70**, 691 (2007)
17. T. Aumann, Eur. Phys. J. A **26**, 441 (2005)
18. A. Tamii, Phys. Rev. Lett. **107**, 062502 (2011)
19. R.-D. Herzberg, *et al.*, Phys. Lett. B **390**, 49 (1997)
20. K. Govaert, *et al*., Phys. Rev. C **57**, 2229 (1998)
21. S. Volz, *et al*., Nucl. Phys. A **779**, 1 (2006)
22. R. Schwengner, *et al.*, Phys. Rev. C **78**, 064314 (2008)
23. D. Savran, *et al*., Phys. Rev. Lett. **100**, 232501 (2008)
24. A.P. Tonchev, *et al*., Phys. Rev. Lett. **104**, 072501 (2010)
25. D. Savran, *et al*., Phys. Rev. Lett. **97**, 172502 (2006)
26. D. Savran, *et al*., Nucl. Phys. A **788**, 165 (2007)
27. J. Endres, *et al*., Phys. Rev. C **80**, 034302, (2009)
28. J. Endres, *et al*., Phys. Rev. Lett. **105**, 212503 (2010)
29. J. Endres, *et al*., Phys. Rev. C **85**, 064331 (2012)
30. J. R. Beene, *et al*., Phys. Rev. C **39**, 1307 (1989)
31. J. R. Beene, *et al*., Phys. Rev. C **41**, 920 (1990)
32. A. Shevchenko, *et al*., Phys. Rev. C **79**, 044305 (2009)
33. A. Richter, Prog. Part. Nucl. Phys. **55**, 387 (2005)
34. H. Aiba, M. Matsuo, S. Nishizaki, and T. Suzuki, Phys. Rev. C **68**, 054316 (2003)
35. H. Aiba and M. Matsuo, Phys. Rev. C **60**, 034307 (1999)
36. D. Lacroix and P. Chomaz, Phys. Rev. C **60**, 064307 (1999)
37. D. Lacroix, *et al*., Phys. Lett. B **479**, 15 (2000)
38. A. Shevchenko, *et al*., Phys. Rev. Lett. **93**, 122501 (2004)
39. A. Shevchenko, *et al*., Phys. Rev. C **77**, 024302 (2008)
40. G. Puglierin, Nucl. Phys. A **834**, 713c (2010)
41. D. Mengoni, Ph.D. Thesis, Università degli Studi di Padova, Padova, Italy, 2008.
42. S. Akkoyun, A. Algora, B. Alikhani, F. Ameil, G. de Angelis, L. Arnold, A. Astier, A. Atac, Y. Aubert, C. Aufranc, A. Austin, S. Aydin, F. Azaiez, S. Badoer, D. Balabanski, D. Barrientos, G. Baulieu, R. Baumann, D. Bazzacco, F. Beck *et al*., Nucl. Instr. Meth. A **668**, 26 (2012)
43. A. Gadea, *et al*., Nucl. Instr. Meth. A **654**, 88 (2011)
44. A. Bracco, *et al*., Mod. Phys. Lett. A **22**, 2479 (2007)
45. R. Nicolini, *et al*., Nucl. Instr. Meth. A **554**, 582 (2007)
46. N. Ryezayeva, *et al*., Phys. Rev. Lett. **89**, 27 (2002)
47. T. Shizuma, *et al*., Phys. Rev. C **78**, 061303 (2008)
48. D. C. Radford, I. Ahmad, R. Holzmann, R. V. F. Janssens, and T. L. Khoo, Nucl. Instr. Meth. A **258**, 111 (1987)
49. S. Agostinelli, *et al*., Nucl. Instr. Meth. A **506**, 250 (2003)
50. E. Farnea, *et al*., Nucl. Instr. Meth. A **621**, 331 (2010)